



## Search for a Dark Matter annihilation signal from the Sagittarius dwarf galaxy with H.E.S.S.

E. MOULIN<sup>1</sup>, C. FARNIER<sup>2</sup>, J.-F. GLICENSTEIN<sup>1</sup>, A. JACHOLKOWSKA<sup>2</sup>, L. ROLLAND<sup>3</sup>, M. VIVIER<sup>1</sup>,  
FOR THE H.E.S.S. COLLABORATION

<sup>1</sup>DAPNIA/DSM/CEA, CE Saclay, F-91191 Gif-sur-Yvette Cedex, France

<sup>2</sup>Laboratoire de Physique Théorique et Astroparticules, Université Montpellier II, CC 70, Place Eugène Bataillon, F-34095 Montpellier Cedex 5, France

<sup>3</sup>Laboratoire d'Annecy-le-Vieux de Physique des Particules, IN2P3/CNRS, 9 Chemin de Bellevue, BP 110 F-74941 Annecy-le-Vieux Cedex, France

emmanuel.moulin@cea.fr

**Abstract:** Dwarf Spheroidal galaxies are amongst the best targets to search for a Dark Matter (DM) annihilation signal. The annihilation of WIMPs in the center of Sagittarius dwarf spheroidal (Sgr dSph) galaxy would produce high energy  $\gamma$ -rays in the final state. Observations carried out with the H.E.S.S. array of Imaging Atmospheric Cherenkov telescopes are presented. A careful modelling of the Dark Matter halo profile of Sgr dwarf was performed using latest measurements on its structural parameters. Constraints on the velocity-weighted cross section of Dark Matter particles are derived in the framework of Supersymmetric and Kaluza-Klein models.

## Introduction

Astrophysical and cosmological observations provide a substantial body of evidences for the existence of Cold Dark Matter (CDM) although its nature remains still unknown. It is commonly assumed that CDM is composed of yet undiscovered non-baryonic particles for which plausible candidates are Weakly Interacting Massive Particles (WIMPs). In most theories, candidates for CDM are predicted in theories beyond the Standard Model of particle physics [1]. The annihilation of WIMPs into  $\gamma$ -rays may lead to detectable very high energy (VHE,  $E > 100$  GeV)  $\gamma$ -ray fluxes above background via continuum emission from the hadronization and decay of the cascading annihilation products, predominantly from  $\pi^0$ 's generated in the quark jets. Among the best-motivated CDM candidates are the lightest neutralino  $\tilde{\chi}$  provided by R-parity conserving supersymmetric extensions of the Standard Model [2], and the lightest Kaluza-Klein particle (LKP) [3] in universal extra dimension theories which is most often the first KK mode of the hypercharge gauge boson,  $\tilde{B}^{(1)}$ . The

H.E.S.S. array of Imaging Atmospheric Cherenkov Telescopes (IACTs), designed for high sensitivity measurements in the 100 GeV - 10 TeV energy regime, is a suitable instrument to detect VHE  $\gamma$ -rays and investigate their possible origin.

Dwarf Spheroidal galaxies such as Sagittarius or Canis Major, discovered recently in the Local Group, are among the most extreme DM-dominated environments. Indeed, measurements of roughly constant radial velocity dispersion of stars imply large mass to luminosity ratios [4]. The core of the Sgr dSph at  $l=5.6^\circ$  and  $b=-14^\circ$  in galactic coordinates at a distance of about 24 kpc from the Sun [5]. Latest velocity dispersion measurements on M giant stars with 2MASS yields a mass to light ratio of about 25 [6]. The luminous density profile of Sgr dSph has two components [7]. The compact component, namely the core, is characterized by a size of about 3 pc FWHM, which corresponds to a point-like region for H.E.S.S. This is the DM annihilation region from which  $\gamma$ -ray signal may be expected. A diffuse component is well fitted by a King model with a characteristic size of 1.6 kpc.

We present in this paper the observations of the Sgr dSph galaxy by the H.E.S.S. array of Imaging Atmospheric Cherenkov Telescopes. A careful modeling of the Dark Matter halo using the latest measurements on the structural parameters of Sagittarius is presented to derive constraints on the WIMP velocity-weighted annihilation rate.

## Search for VHE $\gamma$ -rays from observations of Sagittarius dwarf by H.E.S.S.

H.E.S.S. (High Energy Stereoscopic System) has observed the Sgr dSph in June 2006 with zenith angles ranging from  $7^\circ$  to  $43^\circ$  around an average value of  $19^\circ$ . A total of 11 hours of high quality data are available for the analysis after standard selection cuts. After calibration of the raw shower images from PMT signals [8], two independent reconstruction techniques were combined to select  $\gamma$ -ray events and reconstruct their direction and energy. The first one uses the Hillas moment method [9]. The second analysis referred hereafter as “Model Analysis”, is based on the pixel-per-pixel comparison of the shower image with a template generated by a semi-analytical shower development model [10, 11]. The separation between  $\gamma$  candidates and hadrons is done using a combination of the Model goodness-of-fit parameter [11] and the Hillas mean scaled width and length parameters, which results in an improved background rejection [12]. An additional cut on the primary interaction depth is used to improve background rejection.

The on-source signal is defined by integrating all the events with angular position  $\theta$  in a circle around the target position with a radius of  $\theta_{cut}$ . The target position is chosen according to the photometric measurements of the Sgr dSph luminous cusp showing that the position of the center corresponds to the center of the globular cluster M 54 [13]. The target position is thus found to be (RA =  $18^h55^m59.9s$ , Dec =  $-30^d28'59.9''$ ) in equatorial coordinates (J2000.0). The signal coming from Sgr dSph is expected to come from a region of 1.5 pc, about  $30''$ , much smaller than the H.E.S.S. point spread function (PSF). A  $\theta_{cut}$  value of  $0.14^\circ$  suitable for a point-like source was therefore used in the analysis. In case of a Navarro-Frenk-White (NFW) density profile [14] for which  $\rho$  follows  $r^{-1}$

or a cored profile [15] folded with the point spread function (PSF) of H.E.S.S., the integration region allows to retrieve a significant fraction of the expected signal. See Table 1.

No significant  $\gamma$ -ray excess is detected in the sky map. We thus derived the 95% confidence level upper limit on the observed number of  $\gamma$ -rays:  $N_\gamma^{95\% C.L.}$ . The limit is computed knowing the numbers of events in the signal and background regions above the energy of 250 GeV using the Feldman & Cousins method [16] and we obtain:  $N_\gamma^{95\% C.L.} = 56$ . Given the acceptance of the detector for the observations of the Sgr dSph, a 95% confidence level upper limit on the  $\gamma$ -ray flux is also derived:

$$\Phi_\gamma(E_\gamma > 250 \text{ GeV}) < 3.6 \times 10^{-12} \text{ cm}^{-2}\text{s}^{-1} \quad (95\% C.L.) \quad (1)$$

## Predictions of $\gamma$ -ray from Dark Matter annihilations

The  $\gamma$ -ray flux from annihilations of DM particles of mass  $m_{DM}$  accumulating in a spherical DM halo can be expressed in the form:

$$\frac{d\Phi(\Delta\Omega, E_\gamma)}{dE_\gamma} = \frac{1}{4\pi} \underbrace{\frac{\langle\sigma v\rangle}{m_{DM}^2} \frac{dN_\gamma}{dE_\gamma}}_{\text{Particle Physics}} \times \underbrace{\bar{J}(\Delta\Omega)\Delta\Omega}_{\text{Astrophysics}} \quad (2)$$

as a product of a particle physics component with an astrophysics component. The particle physics part contains  $\langle\sigma v\rangle$ , the velocity-weighted annihilation cross section, and  $dN_\gamma/dE_\gamma$ , the differential  $\gamma$ -ray spectrum summed over the whole final states with their corresponding branching ratios. The astrophysical part corresponds to the line-of-sight-integrated squared density of the DM distribution  $J$ , averaged over the instrument solid angle integration region for H.E.S.S. ( $\Delta\Omega = 2 \times 10^{-5}$  sr):

$$\bar{J}(\Delta\Omega) = \frac{1}{\Delta\Omega} \int_{\Delta\Omega} \text{PSF} * \int_{l.o.s} \rho^2(r[s]) ds d\Omega \quad (3)$$

where PSF is the point spread function of H.E.S.S. The mass distribution of the DM halo of Sgr dwarf has been described by plausible models taking into account the best available measurements of the Sgr dwarf galactic structure parameters. We have used two widely different models. The first has a NFW

Halo type	Parameters	J ( $10^{24}\text{GeV}^2\text{cm}^{-5}$ )	Fraction of signal in $\Delta\Omega = 2 \times 10^{-5}\text{sr}$
Cusped NFW halo	$r_s = 0.2 \text{ kpc}$ $A = 3.3 \times 10^7 M_\odot$	2.2	93.6%
Cored halo	$r_c = 1.5 \text{ pc}$ $v_a = 13.4 \text{ km s}^{-1}$	75.0	99.9%

Table 1: Structural parameters for a cusped NFW ( $r_s$ ,  $A$ ) and a cored ( $r_c$ ,  $v_a$ ) DM halo model, respectively. The values of the solid-angle-averaged l.o.s integrated squared DM distribution are reported in both cases for the solid angle integration region  $\Delta\Omega = 2 \times 10^{-5}\text{sr}$ .

cusped profile [14] with the mass density given by:

$$\rho_{NFW}(r) = \frac{A}{r(r+r_s)^2} \quad (4)$$

with  $A$  the normalization factor and  $r_s$  the scale radius taken from [15]. Using Eq. 3, the value of  $\bar{J}$  obtained with this model is reported in Table 1. We have also studied a core-type halo model as in [15] characterized by the mass density:

$$\rho_{core}(r) = \frac{v_a^2}{4\pi G} \frac{3r_c^2 + r^2}{(r_c^2 + r^2)^2} \quad (5)$$

where  $r_c$  is the core radius and  $v_a$  a velocity scale. However, we have tried to update the  $v_a$  and  $r_c$  values which were used in [15]. By inserting in the Jeans equation the luminosity profile of the Sgr dwarf core of the form:

$$\nu(r) = \frac{\nu_0 r_c^{2\alpha}}{(r_c^2 + r^2)^\alpha} \quad (6)$$

we estimated from the data of [13]  $\alpha = 2.69 \pm 0.10$  and  $r_c = 1.5 \text{ pc}$ . Note that the value of  $r_c$  is only an upper limit. The value of the central velocity dispersion of Sgr Dwarf is  $\sigma = 8.2 \pm 0.3 \text{ km s}^{-1}$  [17]. We have assumed that the velocity dispersion is independent of position. The value of  $v_a$  is then given by  $v_a = \sqrt{\alpha} \sigma = 13.4 \text{ km s}^{-1}$ . The cored model gives a very large value of  $\bar{J}$ , which is reported in Table 1. The third column of Table 1 gives the amount of signal expected in the solid angle integration region  $\Delta\Omega = 2 \times 10^{-5}\text{sr}$ . Fig. 1 shows the limits in the case of a cored (green dashed line) and cusped NFW (red dotted line) profile using the value of  $\bar{J}$  computed above. Predictions for phenomenological MSSM (pMSSM) models are displayed (grey points) as well as those

satisfying in addition the WMAP constraints on the CDM relic density (blue points). The SUSY models are calculated with DarkSUSY4.1 [18]. In the case of a cusped NFW profile, the H.E.S.S. observations do not establish severe constraints on the velocity-weighted cross section. For a cored profile, due to a higher central density, stronger constraints are derived and some pMSSM models

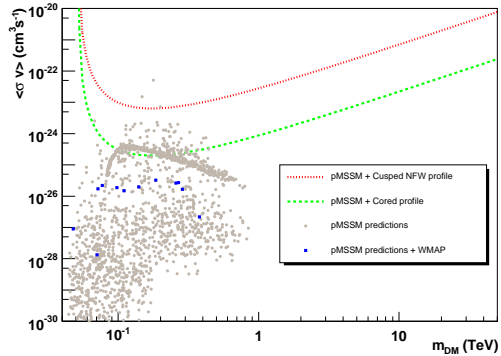


Figure 1: Upper limits at 95% C.L. on  $\langle\sigma v\rangle$  versus the DM particle mass in the case of a cusped NFW (red dotted line) and a cored (green dashed line) DM halo profiles respectively. The pMSSM parameter space was explored with DarkSUSY 4.1 [18], each point on the plot corresponding to a specific model (grey point). Amongst these models, those satisfying in addition the WMAP constraints on the CDM relic density are overlaid as blue square. The limits in case of neutralino dark matter from pMSSM are derived using the parametrisation from [19] for a higgsino-type neutralino annihilation  $\gamma$  profiles.

can be excluded in the upper part of the pMSSM scanned region.

In the case of KK dark matter, the differential  $\gamma$  spectrum is parametrized using Pythia [20] simulations and branching ratios from [3]. Predictions for the velocity-weighted cross section of  $B^{(1)}$  dark matter particle are performed using the formula given in [21]. In this case, the expression for  $\langle\sigma v\rangle$  depends analytically on the  $B^{(1)}$  mass square.

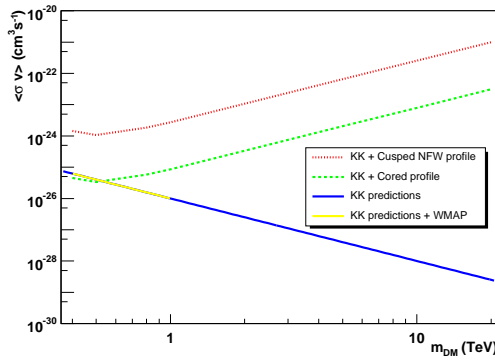


Figure 2: Upper limits at 95% C.L. on  $\langle\sigma v\rangle$  versus the DM particle mass in the  $B^{(1)}$  Kaluza-Klein scenarios for a cusped NFW (red dotted line) and a cored (green dashed line) DM halo profiles respectively. The blue line corresponds to Kaluza-Klein models [3]. Overlaid (yellow line) are the KK models satisfying WMAP constraints on the CDM relic density.

Fig. 2 shows the sensitivity of H.E.S.S. in the case of Kaluza-Klein models where the hypercharge boson  $B^{(1)}$  is the LKP, for a cored (green solid line) and a cusped NFW (red solid line) profile respectively using the value of  $\bar{J}$  computed in section 3.2. With a NFW profile, no Kaluza-Klein models can be tested. In the case of a cored model, some models providing a LKP relic density compatible with WMAP constraints can be excluded. From the sensitivity of H.E.S.S., we exclude  $B^{(1)}$  masses lying in the range 300 - 500 GeV.

## Conclusions

The observations of Sgr dSph with H.E.S.S. reveal no significant  $\gamma$ -ray excess at the nominal target

position. The Sagittarius dwarf DM halo profile has been modeled using latest measurements of its structure parameters. Constraints have been derived on the velocity-weighted cross section of the DM particle in the framework of supersymmetric and Kaluza-Klein models.

## References

- [1] G. Bertone, D. Hooper, J. Silk, Physics Report 405 (2005) 279.
- [2] G. Jungman, K. Kamionkowski, K. Griest, Phys. Rep. 276 (1996) 195.
- [3] G. Servant, T. Tait, Nucl. Phys. B 605 (2003) 391.
- [4] M. I. Wilkinson *et al.*, in: XXI<sup>st</sup> IAP Colloquium : Mass Profiles & Shapes of Cosmological Structures.
- [5] S. Majewski *et al.*, Astroparticle Journal 599 (2003) 1082.
- [6] S. Majewski *et al.*, in: IAU Symposium 220: Dark Matter in Galaxies.
- [7] L. Monaco *et al.*, MNRAS 356 (2006) 1396.
- [8] F. A. Aharonian *et al.*, A&A 22 (2004) 109.
- [9] F. A. Aharonian *et al.*, A&A 430 (2005) 865.
- [10] M. de Naurois *et al.*, in: International Cosmic Ray Conference, 2003.
- [11] M. de Naurois *et al.*, in: Towards a Network of Atmospheric Cherenkov Detectors, 2005.
- [12] F. A. Aharonian *et al.*, A&A 457 (2006) 899.
- [13] L. Monaco *et al.*, MNRAS 356 (2005) 1396.
- [14] J. Navarro, C. Frenk, S. White, Astroparticle Journal 490 (1997) 493.
- [15] N. W. Evans, F. Ferrer, S. Sarkar, Phys. Rev. D 69 (2004) 123501.
- [16] G. Feldman, R. Cousins, Phys. Rev. D 57 (1998) 3873.
- [17] S. Zaggia *et al.*, Mem. Soc. Astr. It. Suppl. 5 (2004) 291.
- [18] P. Gondolo *et al.*, JCAP 0407 (2004) 008.
- [19] L. Bergström, P. Ullio, J. Buckley, Astroparticle Physics 9 (1998) 137.
- [20] PYTHIA package.
- [21] E. Baltz, D. Hopper, JCAP 0507 (2005) 001.